LANGMUIR Article
Cite This: Langmuir 2018, 34, 1767−1774
pubs.acs.org/Langmuir

Accelerated Development of Hippocampal Neurons and Limited Adhesion of Astrocytes on Negatively Charged Surfaces

Mi-Hee Kim,[†] Ji Hun Park,[†] Sunghoon Joo,[†] Daewha Hong,[‡] Matthew Park,[†] Ji Yu Choi,[†] Hye Won Moon,[†] Yang-Gyun Kim,[§] Kyungtae Kang,*[,∥] and Insung S. Choi*[,†]

[†]Center for Cell-Encapsulation Research, Department of Chemistry, KAIST, Daejeon 34141, Korea
[‡]Department of Chemistry and Chemistry Institute of Functional Materials, Pusan National University, Busan 46241, Korea
[§]Department of Chemistry, Sungkyunkwan University, Suwon, Gyeonggi 16419, Korea
[∥]Department of Applied Chemistry, Kyung Hee University, Yongin, Gyeonggi 17104, Korea

Supporting Information

ABSTRACT: This work examines the development of primary neurons and astrocytes on thoroughly controlled functional groups. Negatively charged surfaces presenting carboxylate (COO^-) or sulfonate (SO_3^-) groups prove beneficial to neuronal behavior, in spite of their supposed repulsive electrostatic interactions with cellular membranes. The adhesion and survival of primary hippocampal neurons on negatively charged surfaces are comparable to or slightly better than those on positively charged (poly-D-lysine-coated) surfaces, and neuritogenesis and neurite outgrowth are accelerated on COO^- and SO_3^- surfaces. Moreover, such favorable influences of the negatively charged surfaces are only seen in neurons but not for astrocytes. Our results indicate that the *in vitro* developmental behavior of primary hippocampal neurons is sophisticatedly modulated by angstrom-sized differences in chemical structure or the charge density of the surface. We believe that this work provides new implications for understanding neuron−material interfaces as well as for establishing new ways to fabricate neuro-active surfaces.

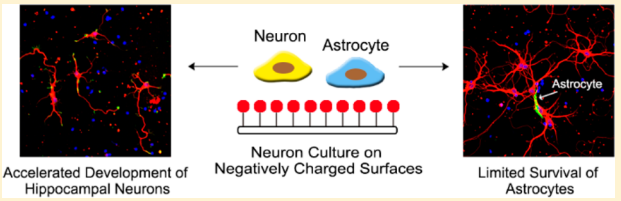

INTRODUCTION

Macromolecules containing amino groups, such as polylysine and polyornithine, have been frequently used as coating materials for *in vitro* neuronal substrates, as electrostatic attraction between the positive charges of the NR_3^+ groups on a culture substrate and the negatively charged neuronal membranes has been suggested as an indispensable factor for stable neuronal adhesion and proper development.[1] This argument has been supported by many previous reports showing that positively charged (e.g., NR_3^+) surfaces were more permissive and compatible to the adhesion and outgrowth of primary neurons compared with negatively charged (e.g., COO^-) and neutral (e.g., CH_3 or zwitterionic) surfaces.[2−7] Neurons *in vivo*, however, face and respond to more than positively charged chemical moieties; various functional groups and local charges present in the extracellular matrix (ECM) and diffusible chemotropic factors released from other cells (e.g., neurotransmitters, netrin, semaphorin, etc.) delicately modulate and guide neuronal behaviors (e.g., neuritogenesis and neurite outgrowth).[8] In this sense, this gap between the commonly used NR_3^+ surfaces and *in vivo* conditions demands detailed investigation of the effects of chemical identities on neuronal behaviors *in vitro* in order to construct *in vivo*-mimetic surfaces as well as understand neuronal environments *in vivo*. Therefore, in this work, we systematically varied surface-functional groups at the molecular level, in a way that has not been pursued conventionally, and observed that contrary to common belief, hippocampal neurons cultured on well-controlled negatively charged carboxylate (COO^-) and sulfonate (SO_3^-) surfaces exhibited developmental behaviors similar to those on ECM glycoproteins[9,10] compared with those on positively charged (poly-D-lysine (PDL)-coated and NH_3^+) surfaces. In addition, COO^- surfaces, while promoting neurite outgrowth and neuritogenesis, selectively limited the survival of astrocytes unlike PDL surfaces.

EXPERIMENTAL SECTION

Materials. Glass coverslips with diameters of 12 mm were purchased from Marienfeld (Germany). Reagents for piranha solution (H_2SO_4 and H_2O_2) were purchased from Junsei Chemical Co. (Japan). Organosilanes (3-aminopropyltrimethoxysilane (APTMS), triethoxysilylpropylsuccinic anhydride (TESPSA), glycidoxypropyltrimethoxysilane (GPTMS), and *n*-butyltrimethoxysilane (*n*-BTMS)) were purchased from Gelest, Inc. (USA). 3-Mercaptopropyltriethoxysilane (MPTES), trichloro(1*H*,1*H*,2*H*,2*H*-perfluorooctyl)-silane, PDL hydrobromide, poly-L-lysine−fluorescein isothiocyanate (PLL-FITC), peracetic acid solution (32 wt % in dilute acetic acid), succinic anhydride (SA), 2-mercaptoethanol, paraformaldehyde, anti-beta-tubulin III antibody produced in rabbit, anti-vinculin antibody produced in rabbit, and anti-glial fibrillary acidic protein (GFAP)

Received: September 5, 2017
Revised: December 16, 2017
Published: December 26, 2017

DOI: 10.1021/acs.langmuir.7b03132
Langmuir 2018, 34, 1767−1774

antibody produced in mouse were purchased from Sigma-Aldrich (USA). Neurobasal medium, B-27, GlutaMAX supplement, live/dead viability/cytotoxicity kit, goat anti-rabbit Alexa Fluor 594 antibody, goat anti-mouse Alexa Fluor 488 antibody, and Alexa Fluor 488 phalloidin were purchased from Thermo Fisher Scientific (USA). Hanks' Balanced Salt Solution (HBSS), Dulbecco's Modified Eagle's Medium (DMEM), phosphate-buffered saline (PBS), fetal bovine serum (FBS), and penicillin−streptomycin solution were purchased from WelGENE, Inc. (Korea). SU8 2010 photoresist and SU8 developer were purchased from Microchem (USA). Bovine serum albumin (BSA), mounting solution with 4′,6-diamidino-2-phenylindole (DAPI), and Cell Counting Kit-8 (CCK-8) were purchased from Santa Cruz Biotechnology, Inc. (USA), Vector Laboratories, Inc. (USA), and Dojindo Molecular Technologies, Inc. (USA), respectively. All reagents were used as received without further purification.

Preparation of Molecularly Controlled Chemical Surfaces. All glass coverslips were cleaned by immersing them into piranha solution (7:3 mixture of H_2SO_4 with H_2O_2) for 10 min. After washing with deionized (DI) water, the coverslips were sonicated in DI water for 10 min to remove possible residues of the piranha solution. The coverslips were then washed with DI water three times and dried under a stream of argon. Dried coverslips were stored at 70 °C for 3−4 h. Right before self-assembled monolayer (SAM) formation, all coverslips, including bare coverslips (negative control), were treated with O_2 plasma for 7 min. Coverslips coated with PDL, a conventional substrate for neurons, were prepared by 1 h dipping in aqueous PDL solution (0.1 mg/mL in DI water). To introduce the NH_3^+-functional groups on coverslips, the cleaned glass coverslips were immersed in 1% APTMS in a mixed solution of methanol/1% acetic acid in DI water (95:5 (v:v)) for 1 h. After washing with methanol, the coverslips were dried under a stream of argon and annealed at 100 °C for 20 min. The coverslips were then washed with methanol repeatedly and dried likewise. For the COO^-(NH_2 + SA) surfaces, APTMS-functionalized surfaces were further reacted with 0.2 M SA in anhydrous tetrahydrofuran (THF) overnight, followed by rinsing with THF and DI water. Other COO^--functional groups were introduced on coverslips by dipping in 10% TESPSA in anhydrous toluene (v:v) for 17 h. The coverslips were rinsed with anhydrous toluene, dimethylformamide (DMF), and DI water. To open the ring (SA) in TESPSA, coverslips were immersed in DI water for 1 h and dried. The SH-, OH-, or CH_3-functionalized coverslips were prepared by dipping in 3% MPTES, 20% GPTMS, or 5% *n*-BTMS in anhydrous toluene for 17 h, respectively. All the coverslips were then washed with anhydrous toluene, DMF, and DI water and dried. The GPTMS-reacted surfaces were further reacted with 0.1 M 2-mercaptoethanol in PBS at 45 °C (air temperature) for 17 h to make the OH-terminated GPTMS. The coverslips were washed with PBS and DI water and then dried likewise. To introduce the SO_3^--functional groups on coverslips, the MPTES-functionalized coverslips were oxidized by peracetic acid solution (32 wt % in dilute acetic acid) at 50 °C for 50 min. The oxidized coverslips were rinsed with DI water and dried. All functionalized coverslips were stored at room temperature until used.

Surface Characterizations. Contact angle measurements were performed with a Phoenix 300 apparatus (Surface Electro Optics Co., Korea) equipped with a video camera. The static contact angles of water droplets (7 μL) were measured for more than eight different samples, and we presented the values of average ± standard deviation. X-ray photoelectron spectroscopy (XPS) was performed with a Sigma Probe (Thermo VG Scientific, UK) equipped with a microfocused X-ray monochromator. During the measurements, the base pressure was 10^{-9} Torr. High-resolution spectra were obtained at a resolution of 0.05 eV from 10 to 30 scans. Zeta-potential measurements were performed at pH 7.4 (pH of culture medium) with an ELSZ-1000 (Otsuka Electronics Co., Japan). To measure the surface charges, glass slides (3 × 1 cm) were used for the chemical functionalizations.

Culture of Hippocampal Neurons and Astrocytes. Primary hippocampal neurons were cultured in serum-free conditions. Hippocampi from E-18 fetal pups of Sprague-Dawley rats were triturated in 1 mL of HBSS using a fire-polished Pasteur pipet. The cell suspension was centrifuged for 3 min at 1000 rpm, and the supernatant was discarded. The cell pellet, which remained on the bottom of the tube, was resuspended in Neurobasal medium supplemented with B-27, GlutaMAX, 12.5 μM L-glutamic acid, and penicillin−streptomycin. The suspended cells were then filtered using a cell strainer with 40 μm pores to obtain uniformly distributed single cells. After counting, cells were seeded at a density of 100 or 150 cells mm^{-2} on the prepared surfaces. Cultures were maintained in an incubator (5% CO_2 and 37 °C), and a half of the medium was replaced with fresh culture medium without L-glutamic acid every 3−4 days. In the case of astrocytes, the culture process was the same as above, but DMEM supplemented with 10% FBS and penicillin−streptomycin was used instead of Neurobasal medium. The entire medium was replaced with fresh culture medium every 3−4 days. This study was approved by IACUC (Institutional Animal Care and Use Committee) of KAIST.

Live/Dead Assay of Hippocampal Neurons. At 1 and 14 DIV (days *in vitro*), the neurons cultured on various chemical surfaces were treated with the live/dead staining solution (2 μM calcein acetoxymethyl ester (calcein AM) and 4 μM ethidium homodimer-1 (EthD-1) in PBS) and incubated for 20 min at room temperature. Images of live (green fluorescent) and dead (red fluorescent) cells were obtained with a Ti-inverted fluorescence microscope (Nikon Co., Japan) equipped with a CoolSNAP cf charge-coupled device (CCD) camera (Photometrics, USA). The number of total counted cells (live and dead cells; counted with ImageJ software (NIH, USA)) in a defined area (ca. 12 mm^2) was used as a metric for adhesion ability, and the percentage of live cells in the total counted cells was used to calculate viability. The values of adhesion and viability on each surface were normalized relative to those on PDL surfaces.

Immunocytochemistry. Neurons and astrocytes cultured on each surface were fixed by immersing into 4% paraformaldehyde in PBS at room temperature for 15 min. The fixed cells were washed with PBS three times and then treated with 0.1% Triton X-100 for 10 min to permeabilize the cellular membranes. After washing with PBS three times, the cells were incubated in 6% BSA in PBS for 30 min at room temperature to prevent nonspecific binding of the antibodies and then washed with 1.5% BSA in PBS. Next, the cells were incubated in the prepared primary antibody solution for 1 h at 37 °C or overnight at 4 °C. Anti-beta-tubulin III, anti-vinculin, and anti-GFAP primary antibody solutions were prepared in 1.5% BSA (in PBS) with volume ratios of 1:500, 1:200, and 1:400, respectively. The cells were washed with 1.5% BSA three times and then incubated in a corresponding secondary antibody solution and phalloidin (if needed) for 1 h at room temperature, followed by the PBS washing steps (×3). Goat anti-rabbit Alexa Fluor 594 IgG, goat anti-mouse Alexa Fluor 488 IgG, and Alexa Fluor 488 phalloidin solutions were prepared in 1.5% BSA with volume ratios of 1:500, 1:400, and 1:150, respectively. The immunostained samples were mounted on glass slides by using a mounting solution containing DAPI to stain nuclei. Fluorescence images were taken with a confocal laser-scanning microscope (LSM 700 META, Carl Zeiss, Germany). From the images, the lengths of the longest neurites and area of GFAP expression in astrocytes were measured with Neuron J plugin in ImageJ software. The number of astrocytes was counted in a defined area (1.13 cm^2), and means were obtained from six different glasses.

Microcontact Printing of PLL-FITC on the COO^- Surface. The polydimethylsiloxane (PDMS) stamp was made by soft lithography. A silicon wafer was spin-coated with SU8 2010 photoresist at 1000 rpm for 30 s and then sequentially baked at 65 °C for 1 min and at 95 °C for 4 min. After adding the film mask with the line pattern on the silicon wafer, the wafer was exposed to UV light with a brightness of 20 mW/cm^2 for 7.5 s. The wafer was hard baked at 65 °C for 1 min and 95 °C for 4 min and developed for 4 min in the SU8-developer to achieve a 20 μm thickness mold. The SU8-patterned mold was sequentially washed with isopropyl alcohol (IPA) and DI water. Before casting the PDMS stamp, trichloro(1*H*,1*H*,2*H*,2*H*-perfluorooctyl)-silane was deposited on the mold for 40 min by the vapor deposition method. The PDMS prepolymer and curing agent were mixed and poured on the mold and cured for 5 h at 60 °C. The cured PDMS was peeled off from the mold and cut into 7 × 7 mm stamps for use. The cleaned PDMS stamp was coated in darkness with PLL-FITC by

DOI: 10.1021/acs.langmuir.7b03132
Langmuir 2018, 34, 1767−1774

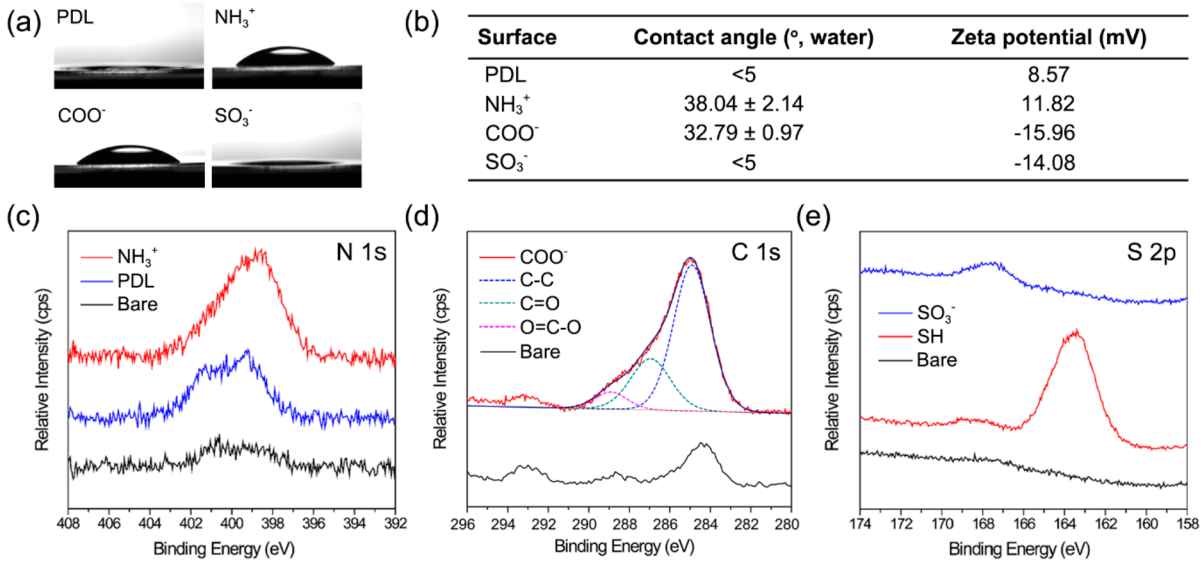

Surface	Contact angle (°, water)	Zeta potential (mV)
PDL	<5	8.57
NH_3^+	38.04 ± 2.14	11.82
COO^-	32.79 ± 0.97	-15.96
SO_3^-	<5	-14.08

Figure 1. (a) Contact angle (water) images of functionalized surfaces. (b) Contact angles (mean ± standard deviation) and zeta-potentials (at pH 7.4). (c–e) XPS spectra: (c) N 1s region of NH_3^+ and PDL surfaces, (d) C 1s region of COO^- surfaces, and (e) S 2p region of SO_3^- surfaces.

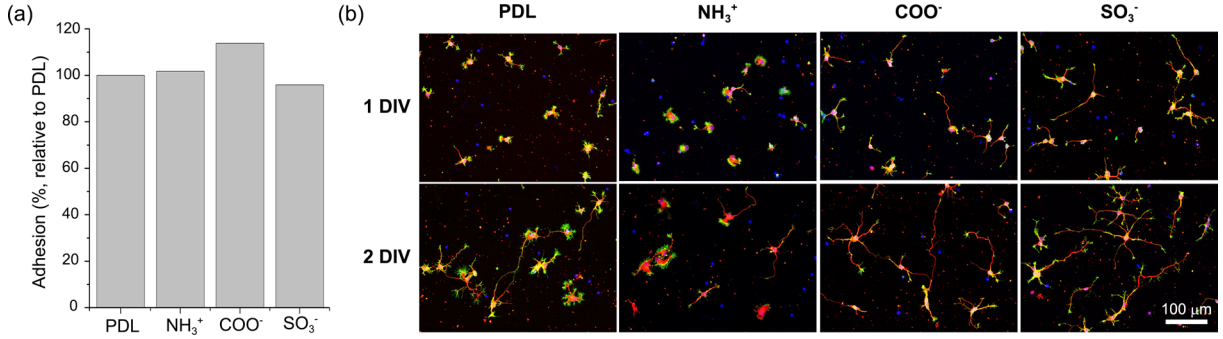

Figure 2. (a) Quantitative analysis of cell adhesion. The number of adhered cells was normalized to that of PDL surfaces for showing relative adhesion. (b) Confocal laser-scanning microscopy (CLSM) micrographs of hippocampal neurons on PDL, NH_3^+, COO^-, and SO_3^- surfaces at 1 and 2 DIV. Cells were stained with anti-beta-tubulin III (red), phalloidin (green), and DAPI (blue), targeting microtubules, actin filaments (lamellipodia/filopodia), and nuclei, respectively.

dropping the PLL-FITC solution (0.1 mg/mL in DI water) on the stamp. After 1 h, the stamp was rinsed with DI water and gently dried under a stream of argon. To print micropatterns on coverslip, a PLL-FITC-coated PDMS stamp was brought in contact with the COO^- coverslip for 10 min under constant pressure (20 g). After removing the stamp, the patterned coverslip was used for hippocampal neuron culture.

RESULTS AND DISCUSSION

Surface Characterizations. Surfaces functionalized with NH_3^+, COO^-, and SO_3^- were generated by forming siloxane self-assembled monolayers (SAMs) on glass coverslips,[11−14] while PDL-coated coverslips were used as a control. After formation of SAMs, each substrate was characterized by water contact angle and zeta-potential measurements, and X-ray photoelectron spectroscopy (XPS) (Figure 1). Characterizations of other molecularly controlled surfaces (bare, OH, SH, and CH_3 surfaces) and neuronal behaviors on them are described in the Supporting Information (Figures S1−S3). Figure 1a shows the static water contact angles (which reflected the differences in their chemical compositions (C, N, O, S, etc.)) of the four chemical surfaces measured with a fixed amount of water droplet (7 μL). PDL and SO_3^- surfaces were very hydrophilic (below 5°), and NH_3^+ and COO^- surfaces were moderately so (38.04 ± 2.14° and 32.79 ± 0.97°, respectively) (Figure 1b). These values were in a good agreement with the published values.[12−14] To get the information on local charge densities, we measured surface charge of the samples at pH 7.4 by zeta-potential measurements (Figure 1b). The zeta-potential of bare surfaces was measured to be −7.14 mV. As expected, the PDL and NH_3^+ surfaces were positively charged, and the COO^- and SO_3^- ones were negatively charged. Quantitatively, the NH_3^+ surfaces (+11.82 mV) were more positively charged than the PDL surfaces (+8.57 mV), presumably because of the higher coating efficiency of NH_3^+-terminated SAMs than the polymer (PDL). The different number of functional groups (two COO^- groups vs one SO_3^- group) might make the COO^- surfaces (−15.96 mV) more negatively charged than SO_3^- surfaces (−14.08 mV).

The XPS analyses further confirmed the successful generation of diverse surface functionalities. In the case of NH_3^+ and PDL surfaces (Figure 1c), the XPS spectra showed an intense peak at the binding energy of 399.0 eV (N 1s), indicating the presence of amines in the films. The spectrum for PDL (blue in Figure 1c) showed another peak at 401.0 eV, attributed to nitrogen from the amide bond.[12,15] As shown in

DOI: 10.1021/acs.langmuir.7b03132
Langmuir 2018, 34, 1767−1774

Figure 1d, the broad C 1s peak for COO^- surfaces was further deconvoluted into three peaks (C−C at 284.9 eV, C═O at 287.0 eV, and O═C−O group at 288.9 eV) according to the molecular structure of the SAMs.[16] We also confirmed the successful formation of SO_3^- SAMs from the XPS spectra of the S 2p region (Figure 1e). The oxidation of SH to SO_3^- led to the peak shift from 163.4 to 167.5 eV (higher binding energy; blue in Figure 1e).[11]

Adhesion and Growth of Hippocampal Neurons on Differently Charged Surfaces. Stable adhesion of neurons on the culture surface is one of the most important prerequisites for their survival and growth. In this respect, we first investigated the influences of the chemical surfaces on neuronal adhesion. We observed that at 1 DIV the adhesion of primary neurons on negatively charged COO^- and SO_3^- surfaces was comparable to or slightly higher than that on PDL surfaces (ca. 114% and 96% for COO^- and SO_3^- surfaces, respectively) (Figure 2a). Viabilities were also comparable for all four substrates (Figure S4). Surprisingly, the neurons cultured on negatively charged surfaces showed accelerated neurite outgrowth and faster axon−dendrite polarization compared with those on PDL surfaces at 1 DIV (Figure 2b). Most neurons on the NH_3^+ surfaces, which were more positively charged than the PDL surfaces, possessed veil-like lamellipodia at 1 DIV, indicating that they were still at early stages of development.

At 2 DIV, the neurons on negatively charged surfaces had much longer neurites in comparison with those on PDL (or NH_3^+) surfaces, indicating accelerated neurite outgrowth and polarization. It is worthy to note that accelerated neurite outgrowth *in vitro* has so far been observed only for certain nanostructures[17−20] and substrates coated with biologically active molecules, such as laminin.[9,10]

Accelerated Development and Stable Network Formation of Hippocampal Neurons on Negatively Charged Surfaces. We quantified neurite outgrowth by measuring the length of the longest neurite for each neuron (Figure 3a and Table S1). At 1 DIV, the difference in the average lengths was not profound (34.65 ± 1.18, 36.48 ± 1.19, and 28.15 ± 0.81 μm for COO^-, SO_3^-, and PDL surfaces, respectively). However, the accelerated neurite outgrowth became clearly discernible at 2 DIV, especially for neurons on SO_3^- surfaces (103.82 ± 4.46 μm vs 67.47 ± 2.51 μm for the PDL surfaces), implying that negatively charged SO_3^- groups had specific (bio)chemical effects on neuronal behavior beyond simple electrostatic interactions. For instance, Hsieh-Wilson et al. reported that chondroitin sulfate (CS) tetrasaccharide, a minimal functional epitope for CS polysaccharides, stimulated the growth and differentiation of hippocampal neurons only when CS was sulfated (O−SO_3^-).[21] It could be inferred that the *in vitro* manipulation of neuronal behaviors required orchestrated chemical functionality, not simply electrostatic interactions; the negatively charged SO_3^- surface might accelerate neurite outgrowth just as sulfated CS stimulated the neuronal growth.

Neuronal development was further investigated by classifying the neurons into three developmental stages (Figure 3b):[17,19] formation of lamellipodia at the cell periphery (stage 1); transformation of lamellipodia into distinct neurites (stage 2); polarization of cell morphology by rapid extension of one neurite (axon) compared with others (dendrites) (stage 3).[22] While most neurons (ca. 85%) belonged to stages 2 and 3 at 1 DIV for negatively charged surfaces, more than 50% of the

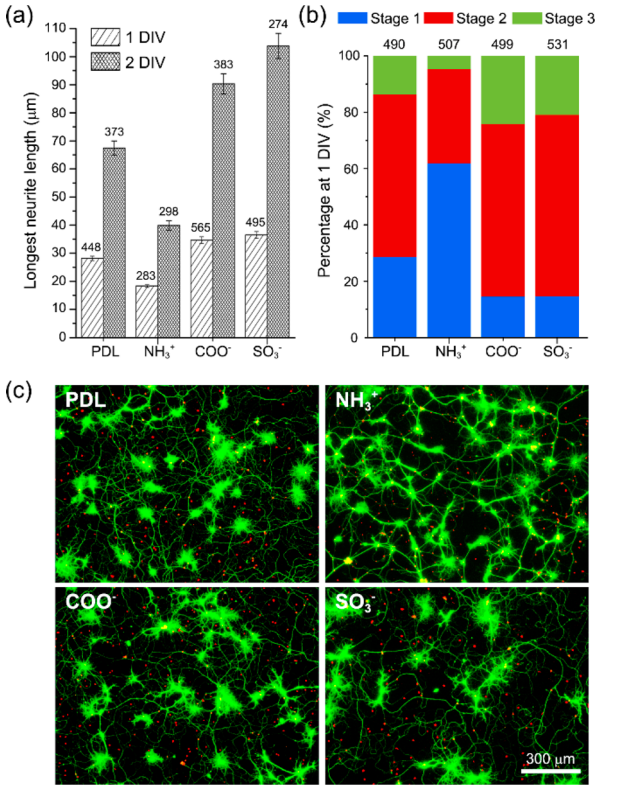

Figure 3. (a) Average lengths of the longest neurites (± standard error) at 1 and 2 DIV and (b) developmental stages of hippocampal neurons on PDL, NH_3^+, COO^-, and SO_3^- surfaces at 1 DIV. The numbers above the bars indicate the numbers of data points. (c) Fluorescence micrographs of neuronal networks at 14 DIV. Cells were stained with calcein acetoxymethyl ester for live cells (green) and ethidium homodimer for dead cells (red).

neurons on NH_3^+ surfaces were still at stage 1, and less than 5% of the neurons reached stage 3, consistent with the results of the neurite-length measurement. When we counted the number of neurites for the neurons classified as stage 2 and 3, the four surfaces did not show significant differences in the populations of uni-, bi-, and multipolar neurons (Figure S5). We also examined the long-term survival of neurons and their network formation at 14 DIV (Figure 3c). The neurons grown on COO^- and SO_3^- surfaces formed stable, interconnected networks with thin layers of neurites and had well-spread and separated somas similar to those on positively charged surfaces.

We supposed that the positively charged groups, electrostatically strengthening the interaction between the neurons and the surfaces, impeded neurite outgrowth, presumably because of overly enhanced adhesion. Negatively charged surfaces in our study, on the other hand, seemed to feature an optimal range of attractive forces for neurite extension and polarization, without compromising neuronal adhesion.[23] A similar balance had been observed previously: laminin, fibronectin, and tenascin glycoproteins were reported to induce accelerated polarization and axonal growth, while decreasing adhesion strength, compared with polyornithine-coated surfaces.[10]

Charge Preference of Hippocampal Neurons and Role of the Terminal Surface Charges. We generated PLL-FITC line patterns on COO^- surfaces (50 μm in width and 50 or 100 μm gaps) by microcontact printing and seeded neurons on the patterned substrates.[24,25] We found that neurons preferred

DOI: 10.1021/acs.langmuir.7b03132
Langmuir 2018, 34, 1767−1774

negatively charged surfaces (the COO^- regions) (Figure 4). Neurites elongated within the COO^- regions, with few crossing

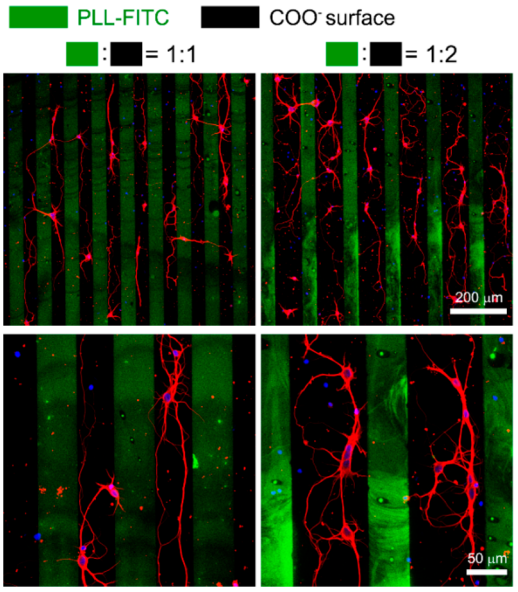

Figure 4. Hippocampal neurons on PLL-FITC line patterns with the COO^- background (50 μm in width and 50 or 100 μm gaps). Negatively charged surfaces were more favorable to neurite outgrowth.

the PLL patterns depending on the incoming angle. The results, thus, indirectly showed how favorable the COO^- surface was for neuronal adhesion and neurite outgrowth, relative to the conventionally used PLL-coated surface.

In order to determine whether the observed neuronal behaviors were the result of the terminal surface charges or the entire surface molecular structure, we varied the backbone structure of the COO^- surface molecules. The amino group on the NH_3^+ surface was reacted with succinic anhydride (SA), leading to a surface-chemical structure composed of the amide bond linkage and a terminal COO^- group ($COO^-(NH_2$ + SA)). The biochemical analyses showed that neurons on $COO^-(NH_2$ + SA) surfaces developed similarly to those on COO^- surfaces (i.e., normal adhesion and high cell viability at 1 DIV, accelerated neurite outgrowth and polarization at 2 DIV, and stable network formation at 14 DIV) (Figure 5). The results, therefore, supported that the observed developmental acceleration of hippocampal neurons was caused by the terminal carboxylate group (or the local negative surface charge).

Limited Adhesion of Astrocytes on Negatively Charged Surfaces. Under the neuro-compatible culture conditions that we used above, neurons were presumed to be present exclusively, but a small number of astrocytes inevitably survived and proliferated depending on factors such as cell seeding density, culture periods, and culture condition. We anticipated that negatively charged surfaces could manipulate the behavior of astrocytes. To observe and quantify individual astrocytes, we stained the GFAP (astrocyte marker) of astrocytes (green) and the microtubules of neurons (red) at 8 DIV, before the active proliferation of astrocytes.

As shown in Figure 6a, contrary to neurons, astrocytes cocultured with neurons were smaller in size and fewer in number on COO^- surfaces than on PDL surfaces; 15% of astrocytes survived on COO^- surfaces relative to those on PDL surfaces, and the average area of GFAP expression was also reduced on COO^- surfaces, at 485.44 ± 52.74 μm^2 compared with 811.78 ± 39.85 μm^2 on PDL surfaces (Figure 6b). The lower population numbers and limited growth of astrocytes continued on COO^- surfaces at 14 DIV, even after proliferation (Figure S6). Furthermore, the survival of astrocytes was also suppressed on the SO_3^- surface, another negatively charged surface, in a good agreement with the COO^- surface (Figure S7).

When astrocytes were cultured under astroglia-compatible conditions (where neurons could not survive), 30% of the astrocytes survived on COO^- surfaces relative to the number on PDL surfaces (Figure S8), consistently reflecting the inhibitory effects of the COO^- surface for astroglial growth. These results indicated that chemical surfaces could modulate cellular behaviors differently among different neural cell types, and the surfaces of negatively charged functional groups would be rather beneficial for neural implants, where selective promotion of neuronal adhesion and outgrowth is often needed.

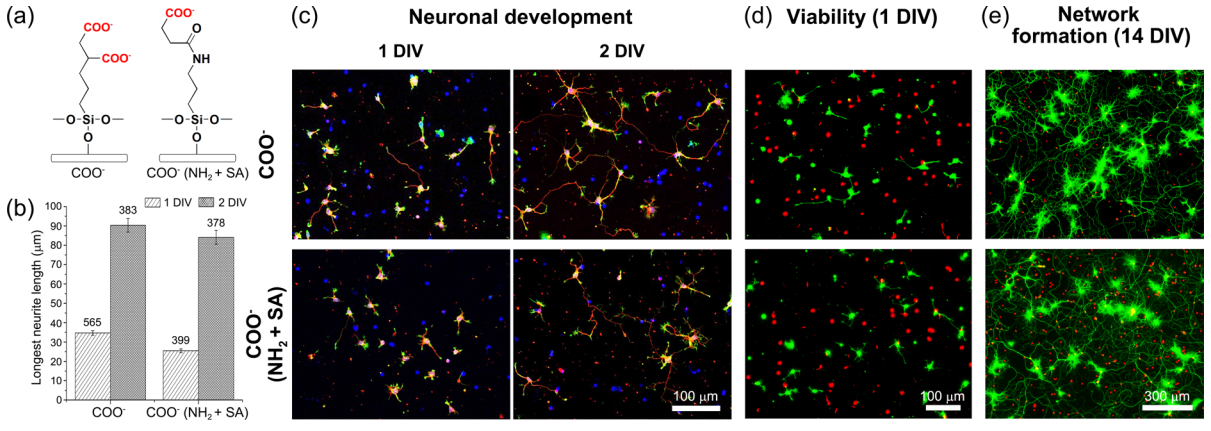

Figure 5. (a) Chemical structures of COO^- and $COO^-(NH_2$ + SA) surfaces. $COO^-(NH_2$ + SA) surfaces were prepared by reacting succinic anhydride (SA) to the NH_3^+ surfaces. (b) Average lengths of the longest neurites (± standard error) on COO^- and $COO^-(NH_2$ + SA) surfaces. (c–e) Development, viability, and network formation of neurons on COO^- and $COO^-(NH_2$ + SA) surfaces. (c) CLSM micrographs of hippocampal neurons at 1 and 2 DIV (red: microtubules; green: actin filaments; blue: nuclei). Fluorescence micrographs of neurons at (d) 1 DIV and (e) 14 DIV (green: live; red: dead).

DOI: 10.1021/acs.langmuir.7b03132
Langmuir 2018, 34, 1767–1774

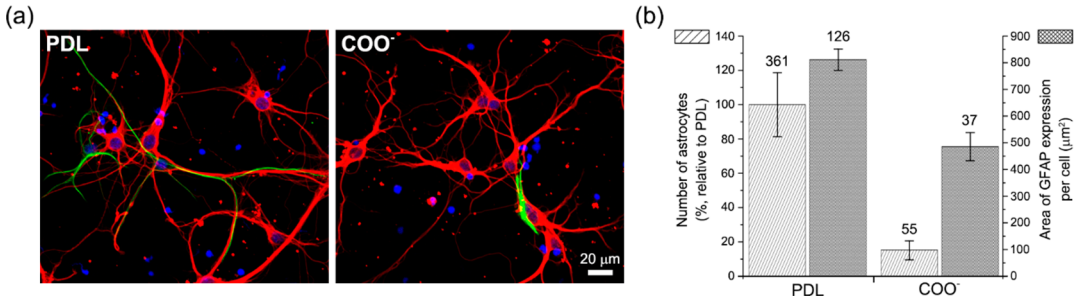

Figure 6. (a) CLSM micrographs of hippocampal neurons (red: microtubules) and astrocytes (green: GFAP expression) on PDL and COO^- surfaces at 8 DIV. (b) Quantitative analyses of the number of astrocytes per substrate and the area of GFAP expression per cell (± standard deviation). The average number of astrocytes on COO^- surfaces was normalized to that on PDL surfaces.

Our results—favorable adhesion and development of neurons on negatively charged surfaces—differ from the previous results showing that COO^--terminated alkanethiol-based SAMs on gold were nonpermissive for neuronal growth.[5] In order to further explore the discrepancy, we cultured hippocampal neurons both on 10-carboxy-1-decanethiol-coated (COO^-) gold surfaces and triethoxysilylpropylsuccinic anhydride-coated (COO^-) glass coverslips under the same culture conditions. Consistent with the previous report, we observed that the gold surfaces were nonpermissive for neuronal adhesion and growth (Figure S9). Considering that our system in this work was based on silane-based SAMs, we hypothesized that such disagreement might originate from differences in local charge density; local charge density would be determined by the effectiveness of molecular packing on surfaces. Even though the ideal packing densities of organosilane SAMs on the native oxides and alkanethiol SAMs on gold are estimated to be roughly similar to each other (5 molecules nm^{-2} vs 4.67 molecules nm^{-2}),[26,27] the practical packing densities of alkanethiols are likely higher than those of organosilanes, resulting in the different local charge densities between them. As a related work, previous studies showed that neural stem cells on organosilane SAMs and alkanethiol SAMs differentiated into different lineages despite the identical functional groups.[14,28]

Astrocytes generally support neuronal growth and function by both contact and noncontact interactions.[29] However, in some cases, balanced growth of neurons and astrocytes is required. For example, there have been efforts to increase the homogeneity of neurons *in vitro* tissue cultures and simultaneously decrease populations of astrocytes because astrocytes continuously proliferate and eventually outnumber the neurons after long-term culture.[30] The complex influence of astrocytes over neurons would interfere with systematic study of neuronal behaviors. To reduce populations of astrocytes, mitotic inhibitors, such as Ara-C (1-β-D-arabinofuranosylcytosine), have been added to culture media[6,7] or serum-free neurocompatible culture media has been used.[31] Moreover, when injured, activated astrocytes form a glial scar at the injury site and inhibit neuronal regeneration by secreting axon-repulsive proteoglycans.[32] To prevent scarring and promote neuronal regeneration, the exploration and development of surfaces or materials[33−35] that suppress growth, proliferation, and activation of astrocytes, while being compatible with neurons, have been of great interest. We found herein that negatively charged COO^- surfaces would be appropriate for this need. Our method has some advantages over previous reports in the following aspects: ease of fabrication, possibility of application to other materials or structures, and selectivity for neural cell types without the addition of inhibitors.

CONCLUSIONS

In summary, we fabricated molecularly controlled 2D surfaces based on organosilane SAMs and analyzed neuronal development with the exclusion of other influences (e.g., ECMs, neurotrophic factors, etc.). The results showed that primary hippocampal neurons adhered favorably to negatively charged surfaces and developed faster than those on PDL-coated surfaces. Negatively charged surfaces in particular had different effects on the behaviors of neurons and astrocytes; neuronal development was accelerated, whereas adhesion of astrocytes was suppressed. While detailed biological mechanisms remain to be established, we believe that our findings emphasize the possibility of the existence of unexplored neuro-compatible or -active functional surfaces that make more sophisticated chemical interactions with hippocampal neurons, beyond simple electrostatic interactions, along with biospecific interactions.[8]

The main purposes of *in vitro* studies on hippocampal neurons would be twofold at least: understanding the biological behaviors of neurons in isolation under less crowded conditions than a brain and providing knowledge and tissue handling technology for applications, such as therapeutic hippocampal transplants. Although this work rather focuses more on the former—fundamental understanding of chemical-functionality effects on *in vitro* neuronal behaviors—it also would provide chemical inspiration for the fabrication of *in vitro* neuro-active scaffolds, in combination with recent studies on the effects of surface nanotopography on neuronal behaviors,[36−40] for the applications.

ASSOCIATED CONTENT

Supporting Information

The Supporting Information is available free of charge on the ACS Publications website at DOI: 10.1021/acs.langmuir.7b03132.

Materials and methods; Table S1: statistical differences in the longest-neurite lengths; Figure S1: characterizations of functionalized surfaces (bare, OH, SH, and CH_3 surfaces); Figure S2: adhesion and viability of neurons on bare, OH, SH, and CH_3 surfaces; Figure S3: neuronal development on bare, OH, and SH surfaces; Figure S4: viability of neurons on PDL, NH_3^+, COO^-, and SO_3^- surfaces; Figure S5: morphological distributions of neurons on various chemical surfaces; Figure S6: hippocampal neurons and astrocytes on PDL and

DOI: 10.1021/acs.langmuir.7b03132
Langmuir 2018, 34, 1767−1774

COO^- surfaces at 14 DIV; Figure S7: hippocampal neurons and astrocytes on PDL and SO_3^- surfaces at 5 DIV; Figure S8: viability and morphology of astrocytes on PDL and COO^- surfaces under astroglia-compatible conditions; Figure S9: live/dead staining of hippocampal neurons on 10-carboxy-1-decanethiol-coated (COO^-) gold surfaces and triethoxysilylpropyl succinic anhydride-coated (COO^-) glass coverslips (PDF)

AUTHOR INFORMATION

Corresponding Authors

*E-mail: ischoi@kaist.ac.kr (I.S.C.).
*E-mail: kkang@khu.ac.kr (K.K.).

ORCID

Insung S. Choi: 0000-0002-9546-673X

Author Contributions

M.-H.K., S.J., K.K., and I.S.C. conceived and designed experiments. M.-H.K., J.H.P., and D.H. prepared various chemical surfaces. M.-H.K., J.H.P., D.H., and Y.-G.K. analyzed various chemical surfaces. M.-H.K., S.J., M.P., J.Y.C., and H.W.M. performed the biological experiments. M.-H.K., J.H.P., Y.-G.K., K.K., and I.S.C. cowrote the paper. All authors commented on the paper.

Notes

The authors declare no competing financial interest.

ACKNOWLEDGMENTS

This work was supported by the Basic Science Research Program through the National Research Foundation of Korea (NRF) funded by the Ministry of Science, ICT & Future Planning (MSIP) (Grants 2012R1A3A2026403, 2015R1A2A2A01008367, and 2016R1C1B2011414).

REFERENCES

(1) Banker, G. A.; Cowan, W. M. Rat Hippocampal Neurons in Dispersed Cell Culture. *Brain Res.* **1977**, *126*, 397−425.
(2) Kleinfeld, D.; Kahler, K. H.; Hockberger, P. E. Controlled Outgrowth of Dissociated Neurons on Patterned Substrates. *J. Neurosci.* **1988**, *8*, 4098−4120.
(3) Stenger, D. A.; Georger, J. H.; Dulcey, C. S.; Hickman, J. J.; Rudolph, A. S.; Nielsen, T. B.; McCort, S. M.; Calvert, J. M. Coplanar Molecular Assemblies of Amino- and Perfluorinated Alkylsilanes: Characterization and Geometric Definition of Mammalian Cell Adhesion and Growth. *J. Am. Chem. Soc.* **1992**, *114*, 8435−8442.
(4) Stenger, D. A.; Pike, C. J.; Hickman, J. J.; Cotman, C. W. Surface Determinants of Neuronal Survival and Growth on Self-Assembled Monolayers in Culture. *Brain Res.* **1993**, *630*, 136−147.
(5) Naka, Y.; Eda, A.; Takei, H.; Shimizu, N. Neurite Outgrowths of Neurons on Patterned Self-Assembled Monolayers. *J. Biosci. Bioeng.* **2002**, *94*, 434−439.
(6) Hu, H.; Ni, Y.; Montana, V.; Haddon, R. C.; Parpura, V. Chemically Functionalized Carbon Nanotubes as Substrates for Neuronal Growth. *Nano Lett.* **2004**, *4*, 507−511.
(7) Tu, Q.; Pang, L.; Chen, Y.; Zhang, Y.; Zhang, R.; Lu, B.; Wang, J. Effects of Surface Charges of Graphene Oxide on Neuronal Outgrowth and Branching. *Analyst* **2014**, *139*, 105−115.
(8) Tessier-Lavigne, M.; Goodman, C. S. The Molecular Biology of Axon Guidance. *Science* **1996**, *274*, 1123−1133.
(9) Lein, P. J.; Banker, G. A.; Higgins, D. Laminin Selectively Enhances Axonal Growth and Accelerates the Development of Polarity by Hippocampal Neurons in Culture. *Dev. Brain Res.* **1992**, *69*, 191−197.
(10) Lochter, A.; Schachner, M. Tenascin and Extracellular Matrix Glycoproteins: From Promotion to Polarization of Neurite Growth *in vitro*. *J. Neurosci.* **1993**, *13*, 3986−4000.
(11) Wang, J.; Yang, S.; Liu, X.; Ren, S.; Guan, F.; Chen, M. Preparation and Characterization of ZrO_2 Thin Film on Sulfonated Self-Assembled Monolayer of 3-Mercaptopropyl Trimethoxysilane. *Appl. Surf. Sci.* **2004**, *221*, 272−280.
(12) Lee, M. H.; Brass, D. A.; Morris, R.; Composto, R. J.; Ducheyne, P. The Effect of Non-Specific Interactions on Cellular Adhesion Using Model Surfaces. *Biomaterials* **2005**, *26*, 1721−1730.
(13) Toworfe, G. K.; Composto, R. J.; Shapiro, I. M.; Ducheyne, P. Nucleation and Growth of Calcium Phosphate on Amine-, Carboxyl- and Hydroxyl-Silane Self-Assembled Monolayers. *Biomaterials* **2006**, *27*, 631−642.
(14) Ren, Y.-J.; Zhang, H.; Huang, H.; Wang, X.-M.; Zhou, Z.-Y.; Cui, F.-Z.; An, Y.-H. *In Vitro* Behavior of Neural Stem Cells in Response to Different Chemical Functional Groups. *Biomaterials* **2009**, *30*, 1036−1044.
(15) Bendali, A.; Agnès, C.; Meffert, S.; Forster, V.; Bongrain, A.; Arnault, J.-C.; Sahel, J.-A.; Offenhäusser, A.; Bergonzo, P.; Picaud, S. Distinctive Glial and Neuronal Interfacing on Nanocrystalline Diamond. *PLoS One* **2014**, *9*, e92562.
(16) Chen, R.; Qu, H.; Guo, S.; Ducheyne, P. The Design and Synthesis of a Soluble Composite Silica Xerogel and the Short-Time Release of Proteins. *J. Mater. Chem. B* **2015**, *3*, 3141−3149.
(17) Cho, W. K.; Kang, K.; Kang, G.; Jang, M. J.; Nam, Y.; Choi, I. S. Pitch-Dependent Acceleration of Neurite Outgrowth on Nanostructured Anodized Aluminum Oxide Substrates. *Angew. Chem., Int. Ed.* **2010**, *49*, 10114−10118.
(18) Gertz, C. C.; Leach, M. K.; Birrell, L. K.; Martin, D. C.; Feldman, E. L.; Corey, J. M. Accelerated Neuritogenesis and Maturation of Primary Spinal Motor Neurons in Response to Nanofibers. *Dev. Neurobiol.* **2010**, *70*, 589−603.
(19) Kang, K.; Choi, S.-E.; Jang, H. S.; Cho, W. K.; Nam, Y.; Choi, I. S.; Lee, J. S. *In Vitro* Developmental Acceleration of Hippocampal Neurons on Nanostructures of Self-Assembled Silica Beads in Filopodium-Size Ranges. *Angew. Chem., Int. Ed.* **2012**, *51*, 2855−2858.
(20) Baranes, K.; Shevach, M.; Shefi, O.; Dvir, T. Gold Nanoparticle-Decorated Scaffolds Promote Neuronal Differentiation and Maturation. *Nano Lett.* **2016**, *16*, 2916−2920.
(21) Tully, S. E.; Mabon, R.; Gama, C. I.; Tsai, S. M.; Liu, X.; Hsieh-Wilson, L. C. A Chondroitin Sulfate Small Molecule that Stimulates Neuronal Growth. *J. Am. Chem. Soc.* **2004**, *126*, 7736−7737.
(22) Dotti, C. G.; Sullivan, C. A.; Banker, G. A. The Establishment of Polarity by Hippocampal Neurons in Culture. *J. Neurosci.* **1988**, *8*, 1454−1468.
(23) Lochter, A.; Taylor, J.; Braunewell, K.-H.; Holm, J.; Schachner, M. Control of Neuronal Morphology *In Vitro*: Interplay Between Adhesive Substrate Forces and Molecular Instruction. *J. Neurosci. Res.* **1995**, *42*, 145−158.
(24) Joo, S.; Kang, K.; Nam, Y. *In Vitro* Neurite Guidance Effects Induced by Polylysine Pinstripe Micropatterns with Polylysine Background. *J. Biomed. Mater. Res., Part A* **2015**, *103*, 2731−2739.
(25) Liu, W.; Xing, S.; Yuan, B.; Zheng, W.; Jiang, X. Change of Laminin Density Stimulates Axon Branching via Growth Cone Myosin II-Mediated Adhesion. *Integr. Biol.* **2013**, *5*, 1244−1252.
(26) Wasserman, S. R.; Whitesides, G. M.; Tidswell, I. M.; Ocko, B. M.; Pershan, P. S.; Axe, J. D. The Structure of Self-Assembled Monolayers of Alkylsiloxanes on Silicon: A Comparison of Results from Ellipsometry and Low-Angle X-Ray Reflectivity. *J. Am. Chem. Soc.* **1989**, *111*, 5852−5861.
(27) Herrwerth, S.; Eck, W.; Reinhardt, S.; Grunze, M. Factors that Determine the Protein Resistance of Oligoether Self-Assembled Monolayers − Internal Hydrophilicity, Terminal Hydrophilicity, and Lateral Packing Density. *J. Am. Chem. Soc.* **2003**, *125*, 9359−9366.
(28) Yao, S.; Liu, X.; He, J.; Wang, X.; Wang, Y.; Cui, F.-Z. Ordered Self-Assembled Monolayers Terminated with Different Chemical Functional Groups Direct Neural Stem Cell Lineage Behaviors. *Biomed. Mater.* **2016**, *11*, 014107.

DOI: 10.1021/acs.langmuir.7b03132
Langmuir 2018, 34, 1767−1774

(29) Allaman, I.; Bélanger, M.; Magistretti, P. J. Astrocyte-Neuron Metabolic Relationships: for Better and for Worse. *Trends Neurosci.* **2011**, *34*, 76−87.
(30) Nam, Y.; Brewer, G. J.; Wheeler, B. C. Development of Astroglial Cells in Patterned Neuronal Cultures. *J. Biomater. Sci., Polym. Ed.* **2007**, *18*, 1091−1100.
(31) Brewer, G. J.; Torricelli, J. R.; Evege, E. K.; Price, P. J. Optimized Survival of Hippocampal Neurons in B27-Supplemented Neurobasal, a New Serum-Free Medium Combination. *J. Neurosci. Res.* **1993**, *35*, 567−576.
(32) Silver, J.; Miller, J. H. Regeneration Beyond the Glial Scar. *Nat. Rev. Neurosci.* **2004**, *5*, 146−156.
(33) Krsko, P.; McCann, T. E.; Thach, T.-T.; Laabs, T. L.; Geller, H. M.; Libera, M. R. Length-Scale Mediated Adhesion and Directed Growth of Neural Cells by Surface-Patterned Poly(ethylene glycol) Hydrogels. *Biomaterials* **2009**, *30*, 721−729.
(34) Capeletti, L. B.; Cardoso, M. B.; dos Santos, J. H.; He, W. Hybrid Thin Film Organosilica Sol-Gel Coatings To Support Neuronal Growth and Limit Astrocyte Growth. *ACS Appl. Mater. Interfaces* **2016**, *8*, 27553−27563.
(35) Wong, D. Y.; Hollister, S. J.; Krebsbach, P. H.; Nosrat, C. Poly(ε-caprolactone) and Poly(L-lactic-*co*-glycolic acid) Degradable Polymer Sponges Attenuate Astrocyte Response and Lesion Growth in Acute Traumatic Brain Injury. *Tissue Eng.* **2007**, *13*, 2515−2523.
(36) Corey, J. M.; Lin, D. Y.; Mycek, K. B.; Chen, Q.; Samuel, S.; Feldman, E. L.; Martin, D. C. Aligned Electrospun Nanofibers Specify the Direction of Dorsal Root Ganglia Neurite Growth. *J. Biomed. Mater. Res., Part A* **2007**, *83*, 636−645.
(37) Ferrari, A.; Cecchini, M.; Dhawan, A.; Micera, S.; Tonazzini, I.; Stabile, R.; Pisignano, D.; Beltram, F. Nanotopographic Control of Neuronal Polarity. *Nano Lett.* **2011**, *11*, 505−511.
(38) Kang, K.; Yoon, S. Y.; Choi, S.-E.; Kim, M.-H.; Park, M.; Nam, Y.; Lee, J. S.; Choi, I. S. Cytoskeletal Actin Dynamics Are Involved in Pitch-Dependent Neurite Outgrowth on Bead Monolayers. *Angew. Chem., Int. Ed.* **2014**, *53*, 6075−6079.
(39) Kang, K.; Park, Y.-S.; Park, M.; Jang, M. J.; Kim, S.-M.; Lee, J.; Choi, J. Y.; Jung, D. H.; Chang, Y.-T.; Yoon, M.-H.; Lee, J. S.; Nam, Y.; Choi, I. S. Axon-First Neuritogenesis on Vertical Nanowires. *Nano Lett.* **2016**, *16*, 675−680.
(40) Park, M.; Oh, E.; Seo, J.; Kim, M.-H.; Cho, H.; Choi, J. Y.; Lee, H.; Choi, I. S. Control over Neurite Directionality and Neurite Elongation on Anisotropic Micropillar Arrays. *Small* **2016**, *12*, 1148−1152.

DOI: 10.1021/acs.langmuir.7b03132
Langmuir 2018, 34, 1767−1774